European Neuropsychopharmacology (▮▮▮▮) ▮, ▮▮▮–▮▮▮

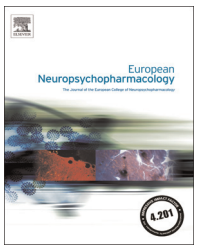

Cellular resilience: 5-HT neurons in Tph2$^{-/-}$ mice retain normal firing behavior despite the lack of brain 5-HT

Alberto Montalbano[a], Jonas Waider[b], Mario Barbieri[c], Ozan Baytas[b], Klaus-Peter Lesch[b], Renato Corradetti[a], Boris Mlinar[a,*]

[a]*Department of Neuroscience, Psychology, Drug Research and Child Health, University of Florence, Florence, Italy*
[b]*Division of Molecular Psychiatry, Laboratory of Translational Neuroscience, Department of Psychiatry, Psychosomatics and Psychotherapy, University of Wuerzburg, Wuerzburg, Germany*
[c]*Department of Medical Sciences, Section of Pharmacology, University of Ferrara, Ferrara, Italy*

Received 21 May 2015; received in revised form 23 July 2015; accepted 27 August 2015

KEYWORDS
Tph2 null mice;
Neuron firing;
Dorsal raphe;
Membrane channels;
I_h;
Electrophysiology

Abstract
Considerable evidence links dysfunction of serotonin (5-hydroxytryptamine, 5-HT) transmission to neurodevelopmental and psychiatric disorders characterized by compromised "social" cognition and emotion regulation. It is well established that the brain 5-HT system is under autoregulatory control by its principal transmitter 5-HT via its effects on activity and expression of 5-HT system-related proteins. To examine whether 5-HT itself also has a crucial role in the acquisition and maintenance of characteristic rhythmic firing of 5-HT neurons, we compared their intrinsic electrophysiological properties in mice lacking brain 5-HT, *i.e.* tryptophan hydroxylase-2 null mice (Tph2$^{-/-}$) and their littermates, Tph2$^{+/-}$ and Tph2$^{+/+}$, by using whole-cell patch-clamp recordings in a brainstem slice preparation and single unit recording in anesthetized animals. We report that the active properties of dorsal raphe nucleus (DRN) 5-HT neurons *in vivo* (firing rate magnitude and variability; the presence of spike doublets) and *in vitro* (firing in response to depolarizing current pulses; action potential shape) as well as the resting membrane potential remained essentially unchanged across Tph2 genotypes. However, there were subtle differences in subthreshold properties, most notably, an approximately 25% higher input conductance in Tph2$^{-/-}$ mice compared with Tph2$^{+/-}$ and Tph2$^{+/+}$ littermates ($p<0.0001$). This difference may at least in part be a consequence of slightly bigger size of the DRN 5-HT neurons in Tph2$^{-/-}$ mice (approximately 10%, $p<0.0001$). Taken together, these findings show that 5-HT neurons acquire and maintain their signature firing properties independently of the presence of their

*Correspondence to: Department of Neuroscience, Psychology, Drug Research and Child Health University of Florence Viale G. Pieraccini 6 50139 Florence Italy. Tel.: +39 0552758277; fax: +39 0552758181.
E-mail address: bmlinar@unifi.it (B. Mlinar).

http://dx.doi.org/10.1016/j.euroneuro.2015.08.021
0924-977X/© 2015 Elsevier B.V. and ECNP. All rights reserved.

Please cite this article as: Montalbano, A., et al., Cellular resilience: 5-HT neurons in Tph2$^{-/-}$ mice retain normal firing behavior despite the lack of brain 5-HT. European Neuropsychopharmacology (2015), http://dx.doi.org/10.1016/j.euroneuro.2015.08.021

principal neurotransmitter 5-HT, displaying an unexpected functional resilience to complete brain 5-HT deficiency.
© 2015 Elsevier B.V. and ECNP. All rights reserved.

1. Introduction

A wide body of evidence links dysfunction of brain serotonin (5-hydroxytryptamine, 5-HT) system to neurodevelopmental and subsequent psychiatric disorders characterized by compromised regulation of "social" cognition and emotion, such as autism or depression and anxiety disorders (see in Booij et al. (2015), Lesch and Waider (2012), Waider et al. (2011)). The output of the 5-HT system is determined by both neurotransmitter specific processes (*i.e.* 5-HT synthesis, degradation, vesicular storage, release and uptake) and the electrophysiological properties of 5-HT neurons, in particular their firing activity. As example, it has been shown that 5-HT tone in the projection areas correlates positively with the firing rate of 5-HT neurons (Crespi, 2009; Sharp et al., 1989, 1990). Distinctive slow and regular action potential firing activity of 5-HT neurons seems not to be specifically associated with any physiological process or environmental factor, but is proportional to the level of behavioral activation across the sleep-wake-arousal cycle (Jacobs and Azmitia, 1992; Trulson and Jacobs, 1979; Wu et al., 2004). Thus, the firing rate of 5-HT neurons depends principally on their intrinsic electrophysiological properties and on tonic, behavioral state-dependent afferent input, such as noradrenergic input which facilitates their firing during wakefulness.

Regulation of 5-HT system function by endogenous 5-HT has been implicated in development as well as in the mature brain. Early studies suggested that during embryonic development, released 5-HT, by direct action on autoreceptors (Branchereau et al., 2002; Huether et al., 1992;Whitaker-Azmitia and Azmitia, 1986) and possibly indirectly, via astroglial cells (Whitaker-Azmitia and Azmitia, 1989) causes an auto-inhibitory effect on the serotonergic neuronal phenotype. Later studies revealed an opposite, trophic developmental role of endogenous 5-HT in which 5-HT/5-HT_{1A} receptors together with brain-derived neurotrophic factor (BDNF)/TrkB receptors constitute an autocrine loop that promotes and maintains differentiation of 5-HT neurons (Eaton et al., 1995; Galter and Unsicker, 2000; Rumajogee et al., 2004). It has been proposed (Rumajogee et al., 2004) that 5-HT has a "biphasic concentration-dependent effect on the regulation of the serotonergic neuronal phenotype, via 5-HT_{1A} receptors. Inhibitory at low concentration, 5-HT would have a trophic effect at higher concentration". A trophic role of 5-HT_{1A} autoreceptors has been further supported by recent evidence for the existence of fibroblast growth factor receptor-1 (FGFR1)-5-HT_{1A} heteroreceptor complexes in the rat midbrain 5-HT neurons (Borroto-Escuela et al., 2015).

In mature brain, 5-HT homeostatically regulates 5-HT system by multiple mechanisms. Specifically, 5-HT acutely limits both its biosynthesis, via end product inhibition of Tph2, and its release, via activation of 5-HT_{1A} and 5-HT_{1B} autoreceptors. Furthermore, endogenous 5-HT autoregulates 5-HT system function on a slower time scale by regulating expression of principal 5-HT-related proteins in 5-HT neurons, *i.e.* Tph2, 5-HT_{1A} and 5-HT_{1B} autoreceptors, and Sert. On the other hand, it is unknown whether CNS 5-HT exerts a similar autoregulatory influence on acquisition and maintenance of intrinsic electrophysiological properties of 5-HT neurons, which underlie the firing rate and are thus a key determinant of the of 5-HT system output. To elucidate this we took advantage of mutant mice with gene-targeted Tph2 inactivation, *i.e.* $Tph2^{-/-}$ mice, which exhibit a complete depletion of the CNS 5-HT and $Tph2^{+/-}$ mice, which exhibit partial reduction in the CNS 5-HT, reaching 20–25% in the rostral raphe (Gutknecht et al., 2012, 2009, 2008). We compared intrinsic electrophysiological properties of dorsal raphe nucleus (DRN) 5-HT neurons in these mice and in wildtype ($Tph2^{+/+}$) littermates, by using whole-cell patch-camp recordings in brainstem slice preparation and single unit recordings in anesthetized animals.

2. Experimental procedures

All animal manipulations were performed according to the European Community guidelines for animal care (DL 116/92, application of the European Communities Council Directive 86/609/EEC) and were approved by the Committee for Animal Care and Experimental Use of the University of Florence and/or by the review board of the Government of Lower Franconia and the University of Würzburg. Animals were housed under standard laboratory conditions (12 h light/dark cycle, ambient temperature 22 ± 1 °C, humidity 40–50%, food and water *ad libitum*).

2.1. Transgenic mice

The generation of $Tph2^{-/-}$ mice and genotyping procedure were described previously (Gutknecht et al., 2008). Generation of 5-HT system specific eGFP expressing mice is detailed in Supplementary methods and illustrated in Supplementary Figure 1.

2.2. Whole-cell patch-clamp recordings

Animals (25–35 days of age) were anesthetized with isoflurane and decapitated. Coronal brainstem slices (200 μm thick) were obtained, incubated and superfused as previously described (Mlinar et al., 2015) and detailed in Supplementary methods. Briefly, slices were superfused in the recording chamber with gassed (95% O_2 and 5% CO_2) artificial cerebrospinal fluid (ACSF) composed of: 124 mM NaCl, 2.75 mM KCl, 1.25 mM NaH_2PO_4, 1.3 mM $MgCl_2$, 2 mM $CaCl_2$, 26 mM $NaHCO_3$, 11 mM D-glucose at a rate of 2 ml min^{-1}. ACSF was warmed (30–32 °C) and supplemented with a cocktail of glutamate and GABA/glycine receptor blockers: 10 μM NBQX (2,3-dioxo-6-nitro-1,2,3,4-tetrahydrobenzo[f]quinoxaline-7-sulfonamide disodium salt), 20 μM DAPV (D-(−)-2-amino-5-phosphonopentanoic acid), 10 mM strychnine hydrochloride, 10 μM SR-95531 (6-imino-3-(4-methoxyphenyl)-1(6H)-pyridazinebutanoic acid hydrobromide) and 2 μM CGP-55845 (3-N[1-(S)-(3,4-dichlorophenyl)ethyl]amino-2-(S)-hydroxypropyl-P-benzyl-phosphinic acid hydrochloride).

Please cite this article as: Montalbano, A., et al., Cellular resilience: 5-HT neurons in $Tph2^{-/-}$ mice retain normal firing behavior despite the lack of brain 5-HT. European Neuropsychopharmacology (2015), http://dx.doi.org/10.1016/j.euroneuro.2015.08.021

Recording pipette solution consisted of: 120 mM K gluconate, 15 mM KCl, 2 mM $MgCl_2$, 10 mM HEPES, 0.1 mM EGTA, 10 mM Na_2 phosphocreatine, 4 mM MgATP, 0.3 mM Na_3GTP (pH 7.35 with KOH). Neurons within dorsal raphe nucleus were visualized by infrared differential interference contrast (IR-DIC) video microscopy with a Newicon camera (C2400-07; Hamamatsu, Hamamatsu City, Japan) mounted on an upright microscope (Axioskop; Zeiss, Göttingen, Germany). Recordings were made using an EPC-10 amplifier (HEKA Elektronic, Lamberecht, Germany). Procedures applied to maximize the accuracy of measurements are detailed in Supplementary methods. Data were analyzed using Fitmaster 2 (HEKA Elektronic), Clampfit 9.2 (Molecular Devices, Sunnyvale, CA, USA) and Prism 5 (GraphPad Software, San Diego, CA, USA).

5-HT neurons were identified using previously established electrophysiological and pharmacological criteria (Audero et al., 2013; Mlinar et al., 2015). Bigger, healthy looking neurons were targeted for the recording. Most of the recorded neurons (>95%) were identified as 5-HT neurons on the basis of characteristic electrophysiological properties displayed in current-clamp mode: half-height width (HHW)>1.1 ms; absent or very small fast afterhyperpolarization; sustained repetitive firing in response to depolarizing current injection. In six experiments in which 5-HT identity of recorded neurons was not certain during the recording, as action potential HHW was in 1.0-1.15 ms range, at the end of the recording response to 5-HT_{1A} receptor agonist 5-carboxamidotryptamine maleate (5-CT; 10 nM) was tested. In all cases, the application of 5-CT produced an increase in $G_{-125/-105\,mV}$ of more than 2 nS, with *I-V* curve consistent with activation of GIRK channels. These neurons were considered 5-HT and included in the group analysis since 5-HT neurons, contrary to non-serotonergic neurons in the DRN, express both 5-HT_{1A} receptors and GIRK channels (del Burgo et al., 2008) and show prominent 5-HT_{1A} receptor-activated GIRK current (Audero et al., 2013; Mlinar et al., 2015).

2.3. *In vivo* electrophysiological recordings

In vivo recordings were done on eleven adult mice (4-5 months) anesthetized with ethyl urethane/chloral hydrate mix (95/5% p/p, 400 mg/kg i.p.) and placed in a stereotaxic frame with digital display (Stoelting Co., Wood Dale, IL, USA). Body temperature was maintained at 37±0.5 °C throughout the experiment utilizing a thermistor-controlled heating pad. Recordings were carried out using glass micropipette (W.P.I., Sarasota, FL, USA) filled with 1.5 M NaCl (impedance 5-15 MΩ). The micropipette was positioned by mean of a hydraulic micropositioner with a digital electronic driver (DKI 650, DKI 607W, David Kopf Instruments, Tujunga, CA, USA) at 4.3-4.8 mm posterior to bregma and 0-0.2 mm laterally from the midline, and then advanced into the DRN, typically found at a depth of 2.0-2.8 mm from dura mater, until a single unit signal was isolated. Putative 5-HT neurons were identified on the basis of their spike duration, analogous to the method we previously used in recordings from the animals of the same genotype *in vitro* (*i.e.* upstroke to downstroke interval, UDI ≥ 0.9 ms) (Gutknecht et al., 2012; Araragi et al., 2013). Different than *in vitro* recordings, discrimination of the neuronal type based on UDI recorded *in vivo* was not always straightforward even in *post-hoc* analysis of average spike since its shape, in particular the position of downstroke peak, was less uniform (*e.g.* see Figure 5A), due to a stronger filtering of the signal and more variable electrode position in respect to the recording neuron. Therefore, to more reliably determine duration of *in vivo* recorded spikes we defined an additional parameter (based on Miyazaki et al. (2011), Sakai (2011)) upstroke to downstroke-half-decay interval ($UD_{HD}I$, Figure 5A), which is less influenced by the filtering of the signal then the UDI. Thus, in recordings *in vivo*, the DRN neurons were presumed 5-HT when their spikes had UDI ≥ 0.9 ms and/or $UD_{HD}I$ ≥ 1.2 ms. Details on the recording procedure are given in Supplementary methods.

2.4. Imaging of eGFP positive 5-HT neurons

Imaging of eGFP positive 5-HT neurons was performed on 30 μm thick coronal serial raphe sections after immunohistochemical labeling of GFP, carried out as detailed in Supplementary methods. Pictures were acquired with an IX81 inverted microscope (Olympus, Germany) for one or two series of Pet1-Cre eGFP:Tph2$^{+/+}$ and Pet1-Cre eGFP:Tph2$^{-/-}$ mice on the same day. For determination 5-HT neuron somatic surface areas, short and long somatic axes were measured in anatomically matched slices in Image J and the surface area was calculated by approximating elliptical shape, *i.e.* area = (short axis/2) × (long axis/2) × Π.

2.5. Expression of potassium channels in raphe neurons

The expression of selected potassium channels (KCNJ2, KCNJ4, KCNJ12, KCNJ14, KCNK2, KCNK3 and KCNK9) in raphe neurons of Tph2$^{-/-}$ and Tph2$^{+/+}$ animals (n=8 per group) was determined using qRT PCR as detailed in Supplementary methods. Analysis of the raw data was performed with LinRegPCR (Ruijter et al., 2009) and values were normalized against the 5 reference genes (Actb; B2m; Tbp; Hprt; and Gapdh) chosen by using the geNorm algorithm (Vandesompele et al., 2002).

2.6. Drugs

Drugs were prepared as stock solutions in distilled water, except CGP-55845 (40 mM stock solution in DMSO, 0.05% final), aliquoted and stored at −20 °C until use. Isoflurane was obtained from Baxter S.p.A. (Rome, Italy); DAP5, SR-95531 and CGP-55845 from Ascent Scientific Ltd. (Bristol, U.K.); DNQX from Abcam (Cambridge, U.K.); ZD-7288 (4-Ethylphenylamino-1,2-dimethyl-6-methylaminopyrimidinium chloride) from Tocris Bioscience (Bristol, UK); HEPES, ATP and DMSO from Fluka (St. Gallen, Switzerland); all other substances were from Sigma-Aldrich.

2.7. Statistical analysis

Statistical analysis was performed using Prism 5 (GraphPad). For comparison of data groups across genotypes ANOVA test with Tukey's multiple comparison post-hoc test was used if distribution was normal (p>0.05) when tested with the D'Agostino and Pearson omnibus normality test. Data groups were considered normally distributed also when p>0.05 was reached following exclusion of one data point in the population. Otherwise, Kruskal-Wallis test with Dunn's multiple comparison post-hoc test was used. In the case of data consisting of two groups (*i.e.* only Tph2$^{+/+}$ and Tph2$^{-/-}$ mice), unpaired *t*-test or Mann-Whitney test were used, as appropriate. The Spearman test was used to assess for correlation between variables. Normally distributed data are reported as mean±SD and non-normally distributed data are reported as median±interquartile range (IQR).

3. Results

3.1. Comparison of passive membrane properties of 5-HT neurons across the genotypes

To examine intrinsic electrophysiological properties of DRN 5-HT neurons whole-cell recordings were done in ACSF supplemented with a mix of synaptic blockers. Under these conditions, 5-HT neurons were silent, *i.e.* no spikes were observed during the initial phase of the recording in loose-seal cell-attached configuration before establishing a tight seal. The

Please cite this article as: Montalbano, A., et al., Cellular resilience: 5-HT neurons in Tph2$^{-/-}$ mice retain normal firing behavior despite the lack of brain 5-HT. European Neuropsychopharmacology (2015), http://dx.doi.org/10.1016/j.euroneuro.2015.08.021

resting membrane potential (RMP) of recorded neurons was determined immediately (2-5 s) after obtaining whole-cell configuration, before dialysis of cell interior with patch pipette solution, and thus closely corresponds to the'real' RMP (see Supplementary methods). As shown in Figure 1A, the RMP of recorded neurons was not different across genotypes ($p=0.78$, ANOVA), having mean$\pm$SD values of: -67.91 ± 8.16 mV in Tph2$^{+/+}$ ($n=46$); -68.02 ± 7.52 mV in Tph2$^{+/-}$ ($n=33$); and -68.90 ± 6.77 mV in Tph2$^{-/-}$ ($n=54$).

Analysis of cell membrane capacitance (C_m), which reflects the surface area of recorded neurons, revealed positively skewed distribution of C_m values, indicative of a subpopulation of larger neurons, particularly evident in Tph2$^{+/-}$ and Tph2$^{-/-}$ mice (Figure 1B). There was a trend toward higher C_m values in Tph2$^{-/-}$ mice (median, IQR: 43.0 pF, 38.1-50.8 pF in Tph2$^{+/+}$; 42.9 pF, 36.0-51.7 pF in Tph2$^{+/-}$; and 46.7 pF, 40.0-54.1 pF in Tph2$^{-/-}$ mice), that did not reach statistical significance as revealed by Kruskal-Wallis test ($p=0.062$).

Upon reaching stable recording conditions, two to three minutes after obtaining whole-cell configuration, the input conductance (G_{CELL}; 1/input resistance) of DRN 5-HT neurons was determined in voltage-clamp by using 10 mV hyperpolarizing pulses from the holding potential of -65 mV. G_{CELL} was not different between Tph2$^{+/+-}$ and Tph2$^{+/-}$ mice, but was significantly greater in Tph2$^{-/-}$ mice compared to both Tph2$^{+/+}$ and Tph2$^{+/-}$ littermates (Figure 1C; $p<0.0001$, ANOVA with Tukey's multiple comparison post-hoc test; mean$\pm$SD values: 1.145 ± 0.284 nS in Tph2$^{+/+}$; 1.095 ± 0.338 nS in Tph2$^{+/-}$; and 1.413 ± 0.353 nS in Tph2$^{-/-}$ mice). This implies increased density of open ion channels at rest in Tph2$^{-/-}$ mice. In contrast, the whole-cell current recorded at -65 mV ($I_{-65\,mV}$), the holding potential in G_{CELL} measurements, was not significantly different across

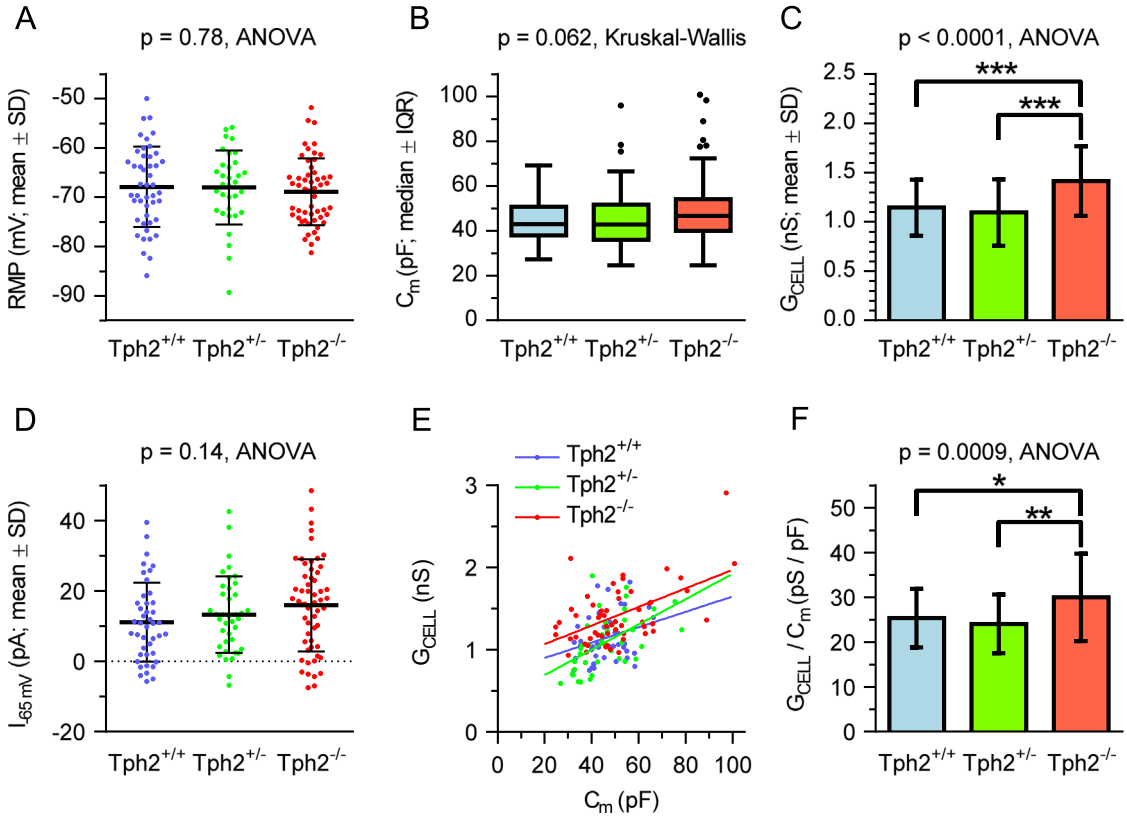

Figure 1 Comparison of 5-HT neuron resting membrane potential and conductance across genotypes. (A) Scatter plot summarizing the resting membrane potential (RMP) of DRN 5-HT neurons. In all three genotypes RMP values were normally distributed ($p=0.80$, 0.12 and 0.37 for Tph2$^{+/+}$, Tph2$^{+/-}$ and Tph2$^{-/-}$, respectively, D'Agostino and Pearson omnibus test). No significant differences were observed. (B) Box plot of cell membrane capacitance (C_m). D'Agostino and Pearson omnibus test revealed normal distribution in Tph2$^{+/+}$ ($p=0.24$, $n=82$) and non-normal distribution in Tph2$^{+/-}$ ($p<0.0001$, $n=68$) and Tph2$^{-/-}$ mice ($p<0.0001$, $n=86$), with a fraction of neurons (outliers) having comparatively higher capacitance. Whiskers represent 1.5 IQR (Tukey). (C) Histogram summarizing the input conductance (G_{CELL}) of DRN 5-HT neurons. The number of neurons is indicated inside bars. ***$p<0.001$, Tukey's multiple comparison post-hoc test. (D) Scatter plot summarizing the steady current at the holding potential ($I_{-65\,mV}$) of DRN 5-HT neurons. No significant differences were observed. (E) The correlation between G_{CELL} and C_m. Symbols represent individual neurons. Lines are best least square fits for respective genotypes. Positive correlation of G_{CELL} with C_m was revealed by correlation analysis (Tph2$^{+/+}$: Spearman $r_s=0.243$, $p=0.12$; Tph2$^{+/-}$: Spearman $r_s=0.627$, $p<0.0001$; Tph2$^{-/-}$: Spearman $r_s=0.397$, $p=0.0024$), indicating higher number of open ion channels at rest in bigger cells. (F) Histogram summarizing the input conductance normalized for the cell membrane capacitance (specific conductance; G_{CELL}/C_m). Error bars represent mean$\pm$SD. The number of neurons is indicated inside bars. *$p<0.05$, **$p<0.01$, Tukey's multiple comparison post-hoc test.

Please cite this article as: Montalbano, A., et al., Cellular resilience: 5-HT neurons in Tph2$^{-/-}$ mice retain normal firing behavior despite the lack of brain 5-HT. European Neuropsychopharmacology (2015), http://dx.doi.org/10.1016/j.euroneuro.2015.08.021

genotypes (Figure 1D; $p=0.14$, ANOVA; normal distribution, $p=0.23$, 0.18 and 0.73 for Tph2$^{+/+}$, Tph2$^{+/-}$ and Tph2$^{-/-}$, respectively, D'Agostino and Pearson omnibus test), having mean$\pm$SD values of: 11.1$\pm$11.2 pA in Tph2$^{+/+}$ ($n=43$); 13.3$\pm$10.9 pA in Tph2$^{+/-}$ ($n=39$); and 15.9$\pm$13.1 pA in Tph2$^{-/-}$ ($n=56$), a finding consistent with the observed lack of difference in RMP across the genotypes.

The observed difference in G_{CELL} could have been due to the difference in the surface areas of recorded neurons, since G_{CELL} in general correlates positively with the cell membrane surface

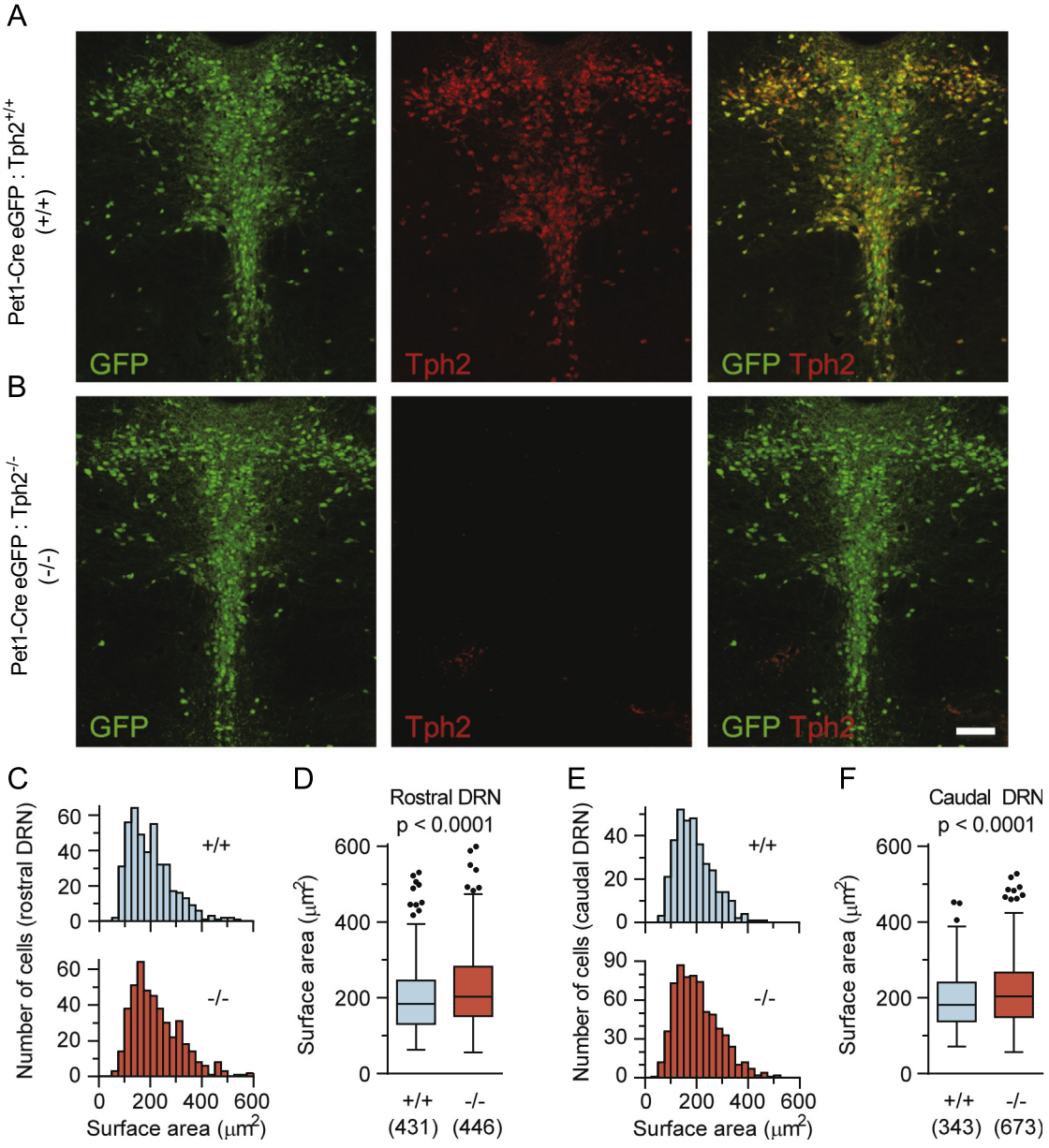

Figure 2 Comparison of 5-HT neuron somatic surface areas in Pet1-Cre eGFP:Tph2$^{+/+}$and Pet1-Cre eGFP:Tph2$^{-/-}$mice. (A,B) Epifluorescent microscopy-obtained images of rostral DRN (-4.6 mm from bregma) of Pet1-Cre eGFP:Tph2$^{+/+}$ (A) and Pet1-Cre eGFP:Tph2$^{-/-}$ mice (B). Scale bar, 100 μm. (C) Histogram representing distribution of rostral DRN (-4.4 to -4.6 mm from bregma) 5-HT neuron somatic surface areas in Pet1-Cre eGFP:Tph2$^{+/+}$ mice (+/+; upper panel) and Pet1-Cre eGFP:Tph2$^{-/-}$ mice ($-/-$; bottom panel). (D) Box plot of rostral DRN 5-HT neuron somatic surface areas in Pet1-Cre eGFP:Tph2$^{+/+}$ (+/+) and Pet1-Cre eGFP:Tph2$^{-/-}$ ($-/-$) mice. $p<0.0001$, Mann-Whitney test. Number of neurons is indicated in parenthesis. Data were obtained from two Pet1-Cre eGFP:Tph2$^{+/+}$ mice and two Pet1-Cre eGFP:Tph2$^{-/-}$ mice. Boxes represent the IQR and the line inside represents the median. Whiskers denote 1.5 IQR (Tukey). (E) Histogram representing distribution of caudal DRN (-4.8 to -4.9 mm from bregma) 5-HT neuron somatic surface areas in Pet1-Cre eGFP:Tph2$^{+/+}$ mice (+/+; upper panel) and Pet1-Cre eGFP:Tph2$^{-/-}$ mice ($-/-$; bottom panel). (F) Box plot of caudal DRN 5-HT neuron somatic surface areas in Pet1-Cre eGFP:Tph2$^{+/+}$ (+/+) and Pet1-Cre eGFP:Tph2$^{-/-}$ ($-/-$) mice. $p<0.0001$, Mann-Whitney test. Number of neurons is indicated in parenthesis. Data were obtained from two Pet1-Cre eGFP:Tph2$^{+/+}$ mice and four Pet1-Cre eGFP:Tph2$^{-/-}$ mice. Boxes represent the IQR and the line inside represents the median. Whiskers denote 1.5 IQR (Tukey).

Please cite this article as: Montalbano, A., et al., Cellular resilience: 5-HT neurons in Tph2$^{-/-}$ mice retain normal firing behavior despite the lack of brain 5-HT. European Neuropsychopharmacology (2015), http://dx.doi.org/10.1016/j.euroneuro.2015.08.021

area. Because correlation analysis revealed positive correlation of G_{CELL} with C_m (Figure 1E; Tph2$^{+/+}$: Spearman r_s=0.243, p=0.12; Tph2$^{+/-}$: Spearman r_s=0.627, p<0.0001; Tph2$^{-/-}$: Spearman r_s=0.397, p=0.0024), we compared specific conductance (input conductance/cell membrane capacitance; G_{CELL}/C_m) of 5-HT neurons across the genotypes. Specific conductance values in all three genotypes were normally distributed (p=0.80, 0.12 and 0.37 for Tph2$^{+/+}$, Tph2$^{+/-}$ and Tph2$^{-/-}$, respectively, D'Agostino and Pearson omnibus test) and, similar to the G_{CELL}, specific conductance resulted not different between Tph2$^{+/+}$ and Tph2$^{+/-}$, but was significantly greater in Tph2$^{-/-}$ mice (Figure 1F; p=0.0009, ANOVA with Tukey's multiple comparison post-hoc test; mean±SD values: 25.37±6.55 pS/pF in Tph2$^{+/+}$; 24.06±6.58 pS/pF in Tph2$^{+/-}$; and 30.00±9.74 pS/pF in Tph2$^{-/-}$ mice). These findings indicate that the observed difference in G_{CELL} of 5-HT neurons across the genotypes reflects a real phenotypic difference, which can be explained only in part by different surface areas of recorded neurons.

3.2. Comparison of 5-HT neuron somatic areas

The observed trend towards higher C_m values in Tph2$^{-/-}$ mice might have been due to a larger 5-HT neuron surface area in Tph2$^{-/-}$ mice, but might have also been a consequence of unrepresentative population sampling, as the choice of the recording neuron in patch-clamp experiments is inherently subjective. To further examine the possibility of larger size of 5-HT neurons in Tph2$^{-/-}$ mice, we compared 5-HT neuron somatic surface areas in two transgenic mouse lines in which 5-HT neuron-specific expression of eGFP was obtained by transgenic Pet1-Cre-mediated recombination, Pet1-Cre eGFP:Tph2$^{+/+}$ (Figure 2A) and Pet1-Cre eGFP:Tph2$^{-/-}$ (Figure 2B). The surface area was calculated from long and short soma axes measurements approximating elliptically shaped somatic surface. Surface areas of all clearly delineated somas were compared in epifluorescent microscopy-obtained images at two matching levels of the DRN: rostral (−4.4 to −4.6 mm from bregma, Figure 2C and D) and caudal (−4.8 to −4.9 mm from bregma, Figure 2E and F). As shown in Figure 2C and D, somatic surface area of rostral DRN 5-HT neurons had non-normal, positively skewed distribution in both mice lines (p<0.0001, D'Agostino and Pearson omnibus test), reminiscent of C_m distribution observed in electrophysiological experiments. Mann–Whitney test revealed significantly larger somatic surface areas in Pet1-Cre eGFP:Tph2$^{-/-}$ (p<0.0001; 10.4% greater median). In caudal DRN (Figure 2G and H), somatic surface areas of 5-HT

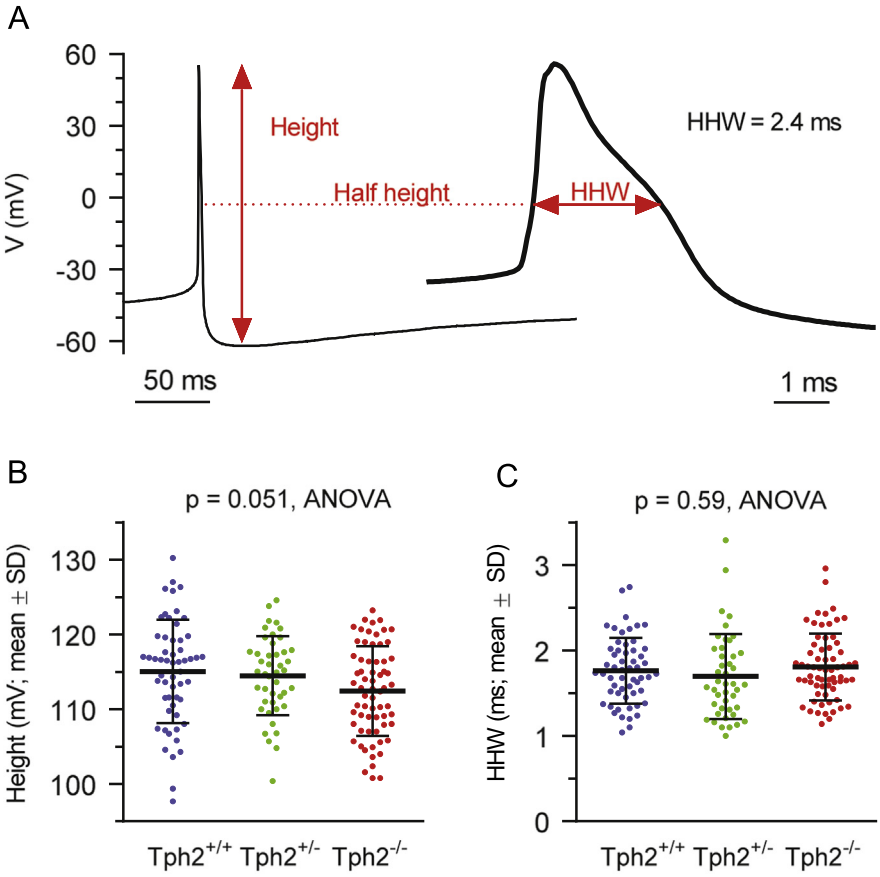

Figure 3 Comparison of 5-HT neuron action potentials. (A) Example of action potential in a DRN 5-HT neuron from Tph2$^{-/-}$ mouse. Trace is average of 20 individual action potentials, evoked with minimal constant current injection (10 pA) sufficient to evoke repetitive firing (0.8 Hz). Right side-the same trace shown on the expanded time scale displays shoulder in a descending phase, characteristic of monoaminergic neurons. HHW=half-height width. (B) Scatter plot summarizing the action potential height in DRN 5-HT neurons. (C) Scatter plot summarizing the action potential HHW in DRN 5-HT neurons. n=56, 44 and 66 for Tph2$^{+/+}$, Tph2$^{+/-}$ and Tph2$^{-/-}$, respectively.

Please cite this article as: Montalbano, A., et al., Cellular resilience: 5-HT neurons in Tph2$^{-/-}$ mice retain normal firing behavior despite the lack of brain 5-HT. European Neuropsychopharmacology (2015), http://dx.doi.org/10.1016/j.euroneuro.2015.08.021

neurons had similar non-normal distribution ($p<0.0001$, D'Agostino and Pearson omnibus test) with significantly larger size in Pet1-Cre eGFP:Tph2$^{-/-}$ mice ($p<0.0001$, Mann–Whitney test; 12.6% greater median). These findings indicate larger size of DRN 5-HT neurons in Tph2$^{-/-}$ mice and suggest that neurons selected for electrophysiological experiments are representative of the overall 5-HT neuron population.

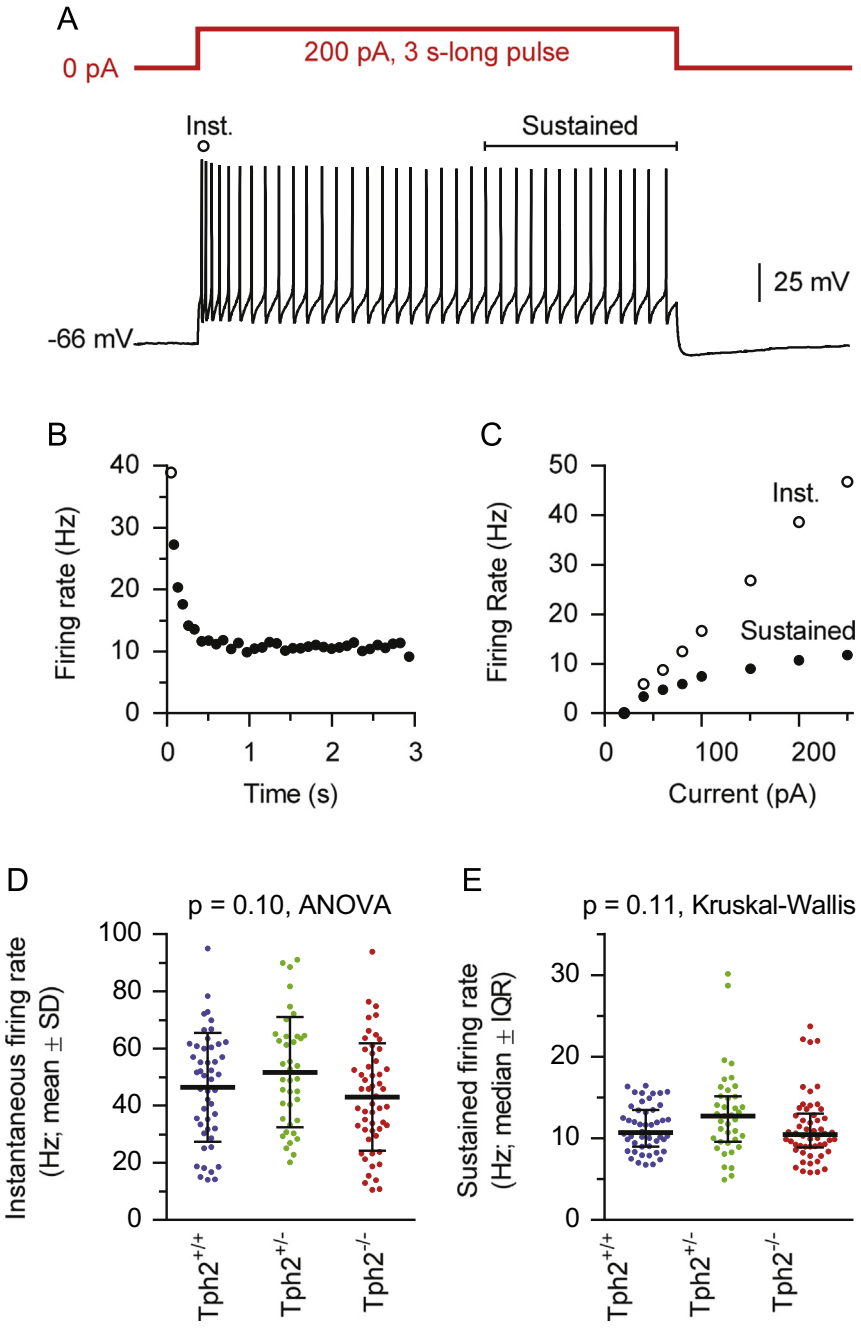

Figure 4 Comparison of 5-HT neuron repetitive firing properties. (A) Example of a whole-cell current clamp recording of a DRN 5-HT neuron used to determine the maximal firing rate. Repetitive firing was evoked by strong (200 pA), three second-long depolarizing somatic current injection (red line). Instantaneous firing rate corresponds to the that of the first two action potentials in the train (open circle). Sustained firing rate was calculated at the last 1.2 s of the pulse (black line). (B) Plot of firing rates between pairs of action potentials shown in A. The firing rate was constant during the second part of the pulse. (C) Input-output relationship (current injection-spike frequency) of the experiment shown in (A, B). Constant current injection of 200 pA evoked near-maximal sustained firing rate. (D) Scatter plot summarizing instantaneous firing rate evoked by 3 s-long, 200 pA pulse across the genotypes. (E) Scatter plot summarizing sustained firing rate evoked by 3 s-long, 200 pA pulse across the genotypes. $n=48$, 39 and 54 for Tph2$^{+/+}$, Tph2$^{+/-}$ and Tph2$^{-/-}$, respectively.

Please cite this article as: Montalbano, A., et al., Cellular resilience: 5-HT neurons in Tph2$^{-/-}$ mice retain normal firing behavior despite the lack of brain 5-HT. European Neuropsychopharmacology (2015), http://dx.doi.org/10.1016/j.euroneuro.2015.08.021

3.3. Action potential and repetitive firing properties of 5-HT neurons *in vitro*

To examine active properties of 5-HT neurons we selected parameters which can be confidently measured in current-clamp whole-cell recordings. We compared action potentials induced by minimal constant-current injections which elicited repetitive firing (see Supplementary methods). Typical for monoaminergic neurons, 5-HT neurons display action potentials with a characteristic shoulder in a descending phase, resulting in long duration action potential, well reflected in its HHW (Figure 3A). As shown in Figure 3B, the height of action potentials was not significantly different across genotypes ($p=0.051$, ANOVA; mean$\pm$SD values: 115.4$\pm$6.9 mV in Tph2$^{+/+}$; 114.5$\pm$5.3 mV in Tph2$^{+/-}$; and 112.4$\pm$6.0 mV in Tph2$^{-/-}$ mice). Comparison of action potential HHW revealed no significant differences across genotypes (Figure 3C; $p=0.59$, ANOVA; mean$\pm$SD values: 1.762$\pm$0.388 ms in Tph2$^{+/+}$; 1.720$\pm$0.549 ms in Tph2$^{+/-}$; and 1.807$\pm$0.390 ms in Tph2$^{-/-}$ mice), suggesting no differences in activity of ion channels underlying action potentials.

We also examined action potential firing in response to depolarizing current injections in current-clamp. 5-HT neurons display sustained firing in response to somatic current injection (Figure 4A and B). We compared responses to 3 s-long, 200 pA pulses, which evoke sustained firing with a near-maximal obtainable firing rate (Figure 4C; see Supplementary methods). There were no significant differences across genotypes in instantaneous firing rate of the first two action potentials (Figure 4D; $p=0.11$, ANOVA; mean$\pm$SD values: 46.4$\pm$19.1 Hz in Tph2$^{+/+}$; 51.7$\pm$19.3 Hz in Tph2$^{+/-}$; and 43.0$\pm$18.8 Hz in Tph2$^{-/-}$ mice) and in sustained firing rate (Figure 4E; $p=0.11$, Kruskal-Wallis; median and IQR values: 10.71 Hz, 8.97-13.45 Hz in Tph2$^{+/+}$; 12.73 Hz, 9.59-15.13 Hz in Tph2$^{+/-}$; and 10.44 Hz, 8.89-13.01 Hz in Tph2$^{-/-}$ mice; Tph2$^{+/+}$: normal distribution $p=0.10$; Tph2$^{+/-}$ and Tph2$^{-/-}$ non-normal distribution, $p=0.0003$ and $p=0.0001$, respectively, D'Agostino and Pearson omnibus test) suggesting no significant change in excitability of 5-HT neurons across the genotypes.

3.4. Comparison of 5-HT neuron firing activity *in vivo*.

We further examined firing properties of the DRN 5-HT neurons in anesthetized animals. Similar to *in vitro* experiments which indicated no changes in action potential of 5-HT neurons in Tph2$^{-/-}$ mice, the shape of their extracellulary recorded spikes *in vivo* appeared normal (e.g.

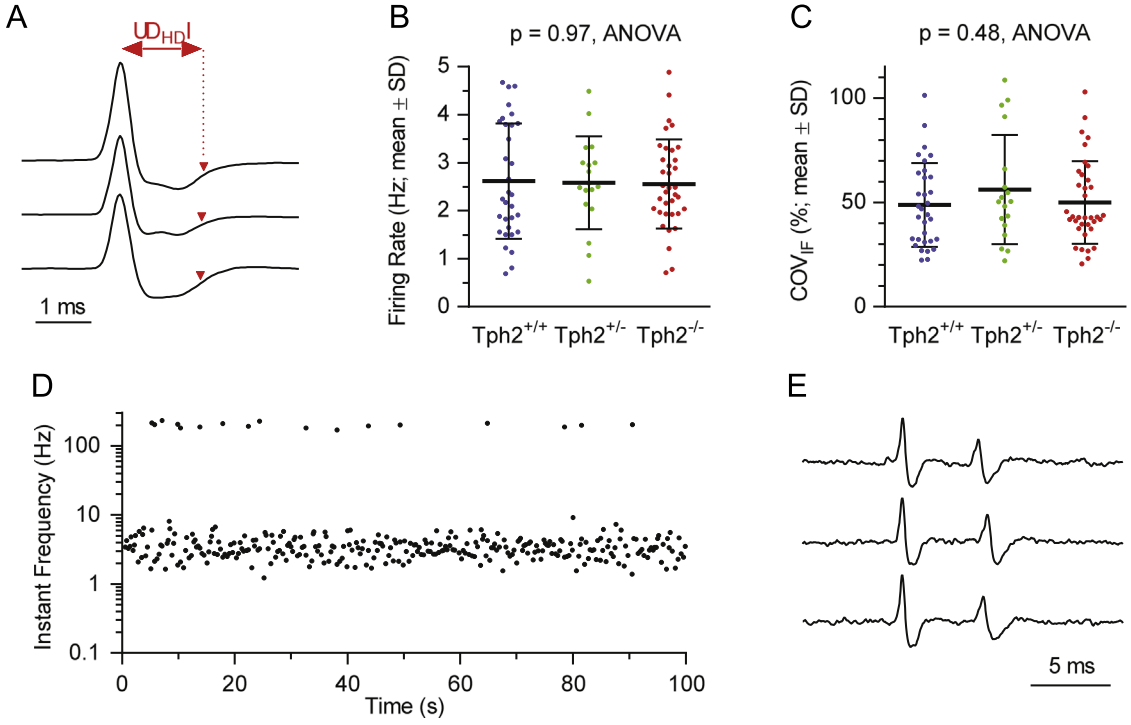

Figure 5 Comparison of 5-HT neuron firing activity in anesthetized animals. (A) Example of spikes of three DRN 5-HT neurons from Tph2$^{-/-}$ mice obtained by extracellular single-unit recording in anesthetized animals. Neurons were considered 5-HT neurons when the interval from the peak of the upstroke to the half-decay of the downstroke (UD$_{HD}$I) was greater than 1.2 ms (see Supplementary methods). Inverted triangles mark half-decay points in spikes of individual neurons. Traces are averages of ~100 individual spikes. (B) Scatter plot summarizing average firing rates of individual 5-HT neurons recorded over the course of 3-10 min. No significant differences were observed across the genotypes. (C) Scatter plot summarizing coefficient of variation of instantaneous firing rate (IF$_{COV}$) of individual 5-HT neurons. No significant differences were observed across the genotypes. (D) Semi-log time plot of instantaneous firing rate of a 5-HT neuron in the DRN of Tph2$^{-/-}$ mouse illustrating firing of doublets (~200 Hz), a characteristic of subpopulation of DRN 5-HT neurons *in vivo*. (E) Traces represent three individual doublets from the experiment shown in (D).

Please cite this article as: Montalbano, A., et al., Cellular resilience: 5-HT neurons in Tph2$^{-/-}$ mice retain normal firing behavior despite the lack of brain 5-HT. European Neuropsychopharmacology (2015), http://dx.doi.org/10.1016/j.euroneuro.2015.08.021

Figure 5A). In order to examine firing activity of 5-HT neurons across the genotypes we compared their firing rates and regularity of firing (coefficient of variance of instantaneous firing rate, IF_{COV}) calculated over the 3-10 min period. As shown in Figure 5B, there was no significant difference across genotypes in average firing rate of DRN 5-HT neurons ($p=0.97$, ANOVA; mean $\pm$ SD values: 2.618 $\pm$ 1.202 Hz in Tph2$^{+/+}$; 2.581 $\pm$ 0.969 Hz in Tph2$^{+/-}$; and 2.554 $\pm$ 0.928 Hz in Tph2$^{-/-}$ mice; Tph2$^{+/+}$: non-normal distribution $p=0.028$; Tph2$^{+/-}$ and Tph2$^{-/-}$ normal distribution, $p=0.69$ and $p=0.57$, respectively, D'Agostino and Pearson omnibus test). Similarly, there was no significant difference in firing regularity, based on comparison of the IF_{COV}. In a subpopulation of 5-HT neurons which fired doublets of action potentials (see below), only the first spike in a doublet was considered for IF_{COV} calculation (Figure 5C; $p=0.48$, ANOVA test; mean $\pm$ SD values: 48.8 $\pm$ 20.0% in Tph2$^{+/+}$; 56.1 $\pm$ 26.2% in Tph2$^{+/-}$; and 49.9 $\pm$ 19.8% in Tph2$^{-/-}$ mice; normal distribution $p=0.22$, 0.29 and 0.08 for Tph2$^{+/+}$, Tph2$^{+/-}$ and Tph2$^{-/-}$, respectively, D'Agostino and Pearson omnibus test). *In vivo*, a subpopulation of 5-HT neurons display firing of spike doublets, or short bursts, with instantaneous frequency in 100-200 Hz range (*i.e.* interspike interval of 5-10 ms) (Hajós et al., 1995, 1996, 2007). As shown in Figure 5D and E, spike doublets were observed in a subpopulation of 5-HT neurons in Tph2$^{-/-}$ mice. Similar proportions of recorded neurons in all three genotypes displayed spike doublets (4 out of 32 in Tph2$^{+/+}$; 4 out of 18 in Tph2$^{+/-}$; and 5 of 36 in Tph2$^{-/-}$ mice) suggesting no significant differences across genotypes. The findings of single-unit recordings *in vivo*, taken together with the findings of current-clamp recordings in brainstem slices, indicate that the CNS 5-HT deficiency does not influence DRN 5-HT neuron firing.

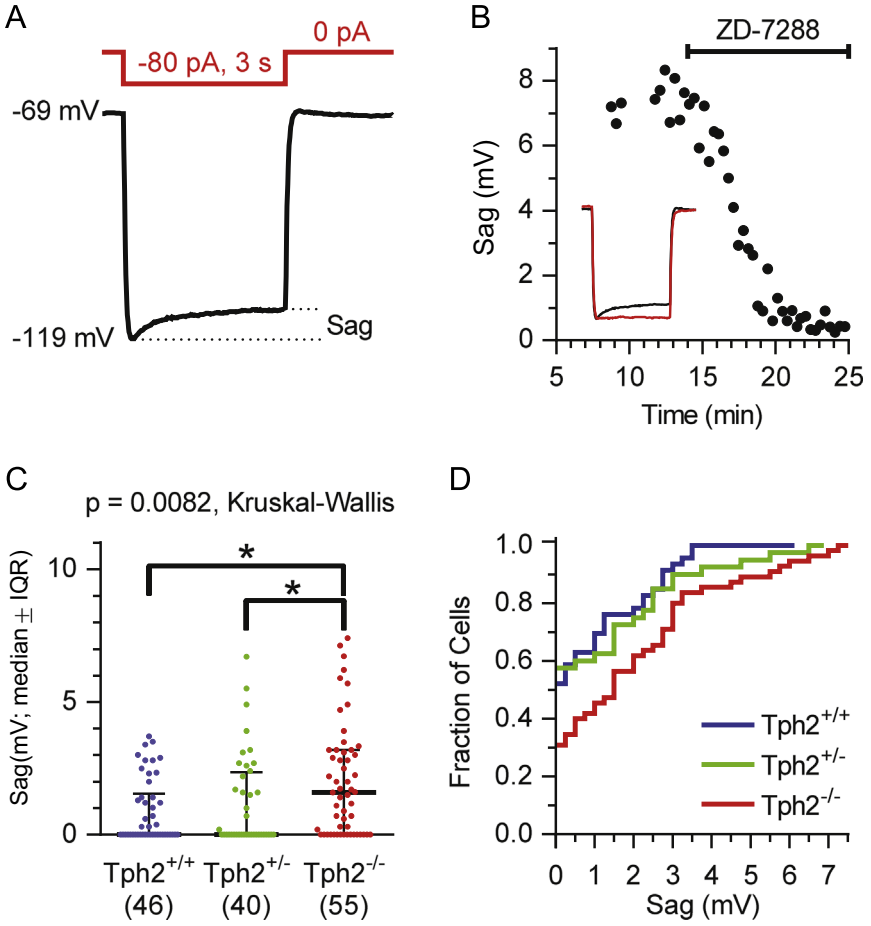

Figure 6 Comparison of HCN channel density. (A) Example of a whole-cell current-clamp recording of a DRN 5-HT neuron used to estimate the density of HCN channels. Voltage responses were evoked by hyperpolarizing somatic current injection (red line), adjusted to hyperpolarize the neuron from the'resting' (holding) potential ranging from -70 to -60 mV to the'peak' potential of -120 to -110 mV. The difference between the peak and the'steady-state' potential at the end (the last 400 ms) of the pulse corresponds to the depolarizing sag. Trace is average of 9 individual responses recorded in a slice obtained from a Tph2$^{-/-}$ mouse. (B) Time-course showing the antagonism of the depolarizing sag following bath application of the HCN channel blocker, ZD-7288 (20 μM), indicating that the sag was caused by the activation of I_h. Inset shows superimposed average traces recorded before (black line, the same trace shown in (A)) and at the last two minutes of ZD-7288 application (red line, average of 7 individual responses). (C) Scatter plot summarizing HCN channels-mediated sag across the genotypes. * $p<0.05$, Dunn's multiple comparison post-hoc test. (D) Cumulative probability histograms of sag amplitudes. Note higher proportion of neurons in Tph2$^{-/-}$ mice displaying the sag.

Please cite this article as: Montalbano, A., et al., Cellular resilience: 5-HT neurons in Tph2$^{-/-}$ mice retain normal firing behavior despite the lack of brain 5-HT. European Neuropsychopharmacology (2015), http://dx.doi.org/10.1016/j.euroneuro.2015.08.021

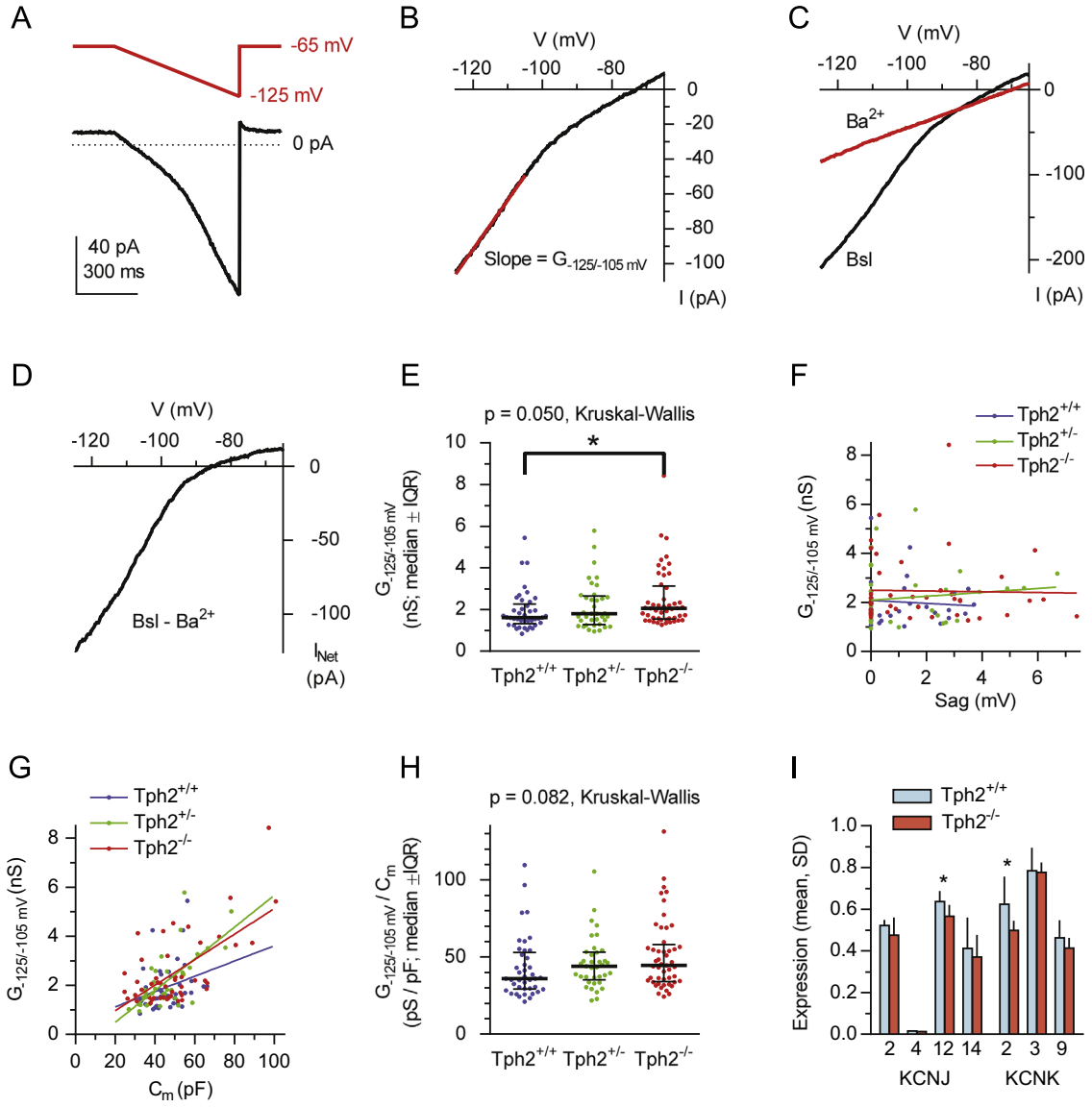

Figure 7 Comparison of responses to hyperpolarizing voltage ramps: increased $G_{-125/-105\,mV}$ in Tph2$^{-/-}$ mice is not due to upregulation of Kir2 channels. (A) Example of a whole-cell voltage clamp recording of a DRN 5-HT neuron from Tph2$^{-/-}$ mouse used to estimate the density of inwardly rectifying K^+ channels. Current responses were evoked by slow hyperpolarizing voltage ramps (100 mV/s) from holding potential of −65 mV to ramp end potential of −125 mV (red line). Trace is average of 7 individual ramps. (B) Current-voltage relationship derived from the ramp shown in (A) (black line). Slope conductance ($G_{-125/-105\,mV}$; red line) was obtained by linear regression of the data over the range of potentials at which K^+ current flows inward (−125 to −105 mV; red line). (C) Example of current-voltage relationships derived from hyperpolarizing ramps of a DRN 5-HT neuron from Tph2$^{-/-}$ mice recorded before (Bsl, black) and after (Ba^{2+}, red) bath application of $BaCl_2$ (150 μM, 5 min), an inwardly rectifying channel blocker. Ba^{2+} abolished inwardly rectifying current component, as visible from near-linear *I-V* recorded in its presence. Traces are averages of 7 individual ramps. (D) Current-voltage plot of net Ba^{2+}-sensitive current (I_{Net}), obtained by subtraction of traces shown in (A). The *I-V* shows rectification and reversal potential characteristic for inwardly rectifying K^+ channels. (E) Scatter plot summarizing $G_{-125/-105\,mV}$ across the genotypes. *$p<0.05$, Dunn's multiple comparison post-hoc test. (non-normal distribution, $p<0.0001$ in Tph2$^{-/-}$ and Tph2$^{+/+}$, $p=0.0004$ in Tph2$^{+/-}$, D'Agostino and Pearson omnibus test). (F) The correlation between $G_{-125/-105\,mV}$ and depolarizing sag (see Figure 5). Symbols represent single experiments. Lines are best least square fits for respective genotypes. There was no correlation of $G_{-125/-105\,mV}$ with the sag amplitude in all genotypes (Tph2$^{+/+}$: Spearman $r_s=-0.023$, $p=0.90$; Tph2$^{+/-}$: Spearman $r_s=0.130$, $p=0.45$; Tph2$^{-/-}$: Spearman $r_s=-0.028$, $p=0.86$). (G) The correlation between $G_{-125/-105\,mV}$ and the cell membrane capacitance (C_m). Symbols represent single experiments. Lines are best least square fits for respective genotypes. Correlation analysis revealed moderate to strong positive correlation of $G_{-125/-105\,mV}$ with C_m in all genotypes (Tph2$^{+/+}$: Spearman $r_s=0.398$, $p=0.0111$; Tph2$^{+/-}$: Spearman $r_s=0.671$, $p<0.0001$; Tph2$^{-/-}$: Spearman $r_s=0.431$, $p=0.0022$). (H) Scatter plot summarizing $G_{-125/-105\,mV}$ normalized for the cell membrane capacitance ($G_{-125/-105\,mV}/C_m$). Non-normal distribution ($p\leq0.0001$ for all genotypes, D'Agostino and Pearson omnibus test). Error bars represent median ± IQR. (I) Comparison of expression of selected K^+ channels in the DRN of Tph2$^{+/+}$ ($n=8$) and Tph2$^{-/-}$ ($n=7$-8) mice. Unpaired *t*-test revealed no differences in expression of KCNJ2 (Kir2.1, $p=0.15$), KCNJ4 (Kir2.3, $p=0.25$), KCNJ14 (Kir2.4, $p=0.54$), KCNK3 (TASK-1, $p=0.84$) and KCNK9 (TASK-3, $p=0.20$), while significance was reached for KCNJ12 (Kir2.2, $p=0.018$) and KCNK2 (TREK-1, $p=0.035$).

3.5. Comparison of 5-HT neuron subthreshold properties across the genotypes

Because 5-HT neurons in Tph2$^{-/-}$ mice had higher G_{CELL}, but unchanged action potential firing, we further examined subthreshold properties in an attempt to identify ion channels underlying higher G_{CELL} in Tph2$^{-/-}$ mice. We compared activities of hyperpolarization-activated cyclic nucleotide-gated cation (HCN) channels, which mediate I_h and inwardly-rectifying potassium (IRK) channels. To compare densities of HCN channels across the genotypes, we measured the depolarizing sag occurring in response to hyperpolarizing pulses in current-clamp mode (Figure 6A; see Supplementary methods). Bath application of the HCN channel blocker, ZD-7288 (20 μM, 10 min) abolished depolarizing sag in all neurons tested (n=3, Tph2$^{-/-}$; n=2, Tph2$^{+/-}$; n=3, Tph2$^{+/+}$) confirming that the sag is due to the activation of I_h (e.g. Figure 6B). Depolarizing sag was non-existent or relatively small in 5-HT neurons from all genotypes, but nevertheless, Kruskal-Wallis test revealed that it was significantly greater in Tph2$^{-/-}$ mice (p=0.0082, Figure 6C). In addition, the proportion of 5-HT neurons expressing the sag was higher in Tph2$^{-/-}$ mice (Figure 6D; sag ≥ 0.5 mV: 65.5% in Tph2$^{-/-}$, 42.5% in Tph2$^{+/-}$, 41.3% in Tph2$^{+/+}$ mice). Finally, there was no significant correlation of the sag amplitude with G_{CELL} in Tph2$^{-/-}$ mice (Spearman r_s = −0.133, n=50, p=0.36).

To compare the activity of IRK channels we used hyperpolarizing voltage ramps (Figure7A) and measured the conductance from the slope of the recorded current in range of potentials from −125 to −105 mV ($G_{-125/-105\,mV}$; Figure. 7B). Bath application of a non-selective blocker of inwardly rectifying K^+ channels, Ba^{2+} ($BaCl_2$ 150 μM, 3-5 min) abolished inwardly rectifying current in all neurons tested (*e.g.* Figure 7C, note the absence of rectification in Ba^{2+}; n=3, 1, 7 for Tph2$^{+/+}$, Tph2$^{+/-}$ and Tph2$^{-/-}$ mice, respectively). The *I-V* of net Ba^{2+}-sensitive current displayed inward rectification and the reversal potential close to that of K^+ (Figure 7D), indicating that it is inwardly-rectifying K^+ current. As shown in Figure 7E, DRN 5-HT neuronal populations in all three genotypes had non-normally distributed $G_{-125/-105\,mV}$ values (median and IQR: 1.615 nS, 1.315-2.269 nS in Tph2$^{+/+}$; 1.802 nS, 1.273-2.644 nS in Tph2$^{+/-}$; 2.054 nS, 1.548-3.125 nS in Tph2$^{-/-}$), with a subpopulation of neurons having distinctively higher $G_{-125/-105\,mV}$ values. Kruskal-Wallis test revealed borderline significant difference in $G_{-125/-105\,mV}$ across the genotypes (p=0.050) and Dunn's multiple comparison post-test showed significant difference only between Tph2$^{-/-}$ and Tph2$^{+/+}$ mice (p<0.05). The slope conductance at hyperpolarized potentials can be in some extent due to I_h. However, correlation analysis indicated that $G_{-125/-105\,mV}$ does not correlate with the sag magnitude in recorded neurons (Figure 7F), confirming that $G_{-125/-105\,mV}$ principally reflects the density of inwardly rectifying K^+ channels. Correlation analysis, however, revealed moderate to strong positive correlation of $G_{-125/-105\,mV}$ with C_m in all genotypes (Tph2$^{+/+}$: Spearman r_s=0.398, p=0.0111; Tph2$^{+/-}$: Spearman r_s=0.671, p<0.0001; Tph2$^{-/-}$: Spearman r_s=0.431, p=0.0022; Figure 7G). Therefore, $G_{-125/-105\,mV}$ data 'normalized' for the cell capacitance, *i.e.* specific $G_{-125/-105\,mV}$ ($G_{-125/-105\,mV}/C_m$) were also compared across genotypes (Figure 7H). Kruskal-Wallis test revealed no significant difference in specific $G_{-125/-105\,mV}$ (p=0.082), suggesting small, if any, difference in the activity of IRK channels across the genotypes. Finally, we compared the expression of IRK (Kir2) type channels in the DRN of Tph2$^{-/-}$ and Tph2$^{+/+}$ mice. In addition, we compared expression KCNK2 (TREK-1), KCNK3 (TASK-1) and KCNK9 (TASK-3), the members of the two-pore-domain (2P) background K^+ channel family which are highly expressed in 5-HT neurons and contribute to their G_{CELL} (Heurteaux et al., 2006; Talley et al., 2001; Washburn et al., 2002) As shown in Figure 7I, there were no marked differences in expression of compared K^+ channels, although significance was reached for KCNJ12 (p=0.018) and KCNK2 (p=0.035), which were on average expressed 9.9% and 20.1% less in Tph2$^{-/-}$ mice, respectively. The finding that the expression of IRK and 2P channels was unchanged or decreased in Tph2$^{-/-}$ mice suggests that increased G_{CELL} in Tph2$^{-/-}$ mice is not due to increased expression of the compared K^+ channels.

4. Discussion

In the present work, we compared electrophysiological properties of DRN 5-HT neurons in Tph2$^{-/-}$ and Tph2$^{+/-}$ mutant mice and in wt (Tph2$^{+/+}$) littermates. No substantial differences in any parameter reflecting their firing activity both *in vivo* and *in vitro* were found. These results provide evidence that 5-HT neurons acquire and maintain their characteristic firing properties independently of the presence of their principal neurotransmitter 5-HT, and display an unexpected resilience toward complete 5-HT deficiency.

The firing activity of the DRN 5-HT neurons was directly assessed by single unit recordings in anesthetized animals. All parameters characterizing firing activity *in vivo* (*i.e.* firing rate; coefficient of variation of instantaneous firing rate and the incidence of spike doublets) were remarkably similar across the genotypes. These findings are consistent with our previous results obtained using loose-seal cell-attached recording in brainstem slices (Araragi et al., 2013; Gutknecht et al., 2012), although in the latter study the firing rate in Tph2$^{-/-}$ mice was found slightly lower than in Tph2$^{+/+}$.

As firing activity of neurons *in vivo* is not necessarily determined exclusively by their intrinsic properties, but it may also be modulated by the afferent neural activity in the intact brain, we further examined properties of 5-HT neurons using whole-cell recordings in brainstem slices. All *in vitro* recordings were done in the presence of a cocktail of GABAergic and glutamatergic synaptic receptor blockers to electrically isolate the recorded 5-HT neuron and thus permit the measurement of its intrinsic electrophysiological properties. Although some differences across Tph2 genotypes were observed in subthreshold properties of 5-HT neurons (discussed below), most of parameters compared, in particular those relevant for excitability and firing behavior (*i.e.* action potential height and half-height width, instantaneous and persistent firing in response to depolarizing current pulses) indicated a lack of substantial differences across the genotypes. Together with findings of *in vivo* experiments, these results indicate that 5-HT neurons acquire and maintain their firing properties despite the complete ablation of endogenous neuronal 5-HT synthesis during adulthood.

In contrast to firing properties of the DRN 5-HT neurons, subtle differences were observed in some of their

Please cite this article as: Montalbano, A., et al., Cellular resilience: 5-HT neurons in Tph2$^{-/-}$ mice retain normal firing behavior despite the lack of brain 5-HT. European Neuropsychopharmacology (2015), http://dx.doi.org/10.1016/j.euroneuro.2015.08.021

subthreshold properties. Particularly, 5-HT neurons in Tph2$^{-/-}$ mice displayed higher G_{CELL} compared to their littermates. The difference was relatively small ($\approx$25%), but resulted highly significant ($p<0.0001$ for both ANOVA and Tukey's post-hoc tests) and is unlikely to be a consequence of differences in cell and/or animal sampling and recording conditions since all recordings were done in stringent conditions (*e.g.* no differences in seal and access resistance; recording temperature; slice viability; age of animals). Increased G_{CELL} in Tph2$^{-/-}$ mice without concomitant change in the RMP as well as in the holding current is somewhat surprising because opening or closing of ion channels responsible for the change in G_{CELL} is expected to simultaneously change the holding current and the RMP. The simplest way to produce the observed increase in G_{CELL} without a simultaneous change in the RMP is by opening of at least two different ion channel types in 5-HT neurons in Tph2$^{-/-}$ mice. As example, opening of a potassium channel (which hyperpolarizes the cell membrane) together with opening of a sodium channel or a non-selective cation channel (which depolarize the cell membrane) could increase G_{CELL} without affecting the RMP. Although such a mechanism cannot be excluded, it seems unlikely because there was no increase in subthreshold K^+ conductances in Tph2$^{-/-}$ mice. Alternatively, small increase in intracellular Ca^{2+} concentration, *e.g.* by increased influx through HCN channels, may in turn increase Ca^{2+}-activated K^+ current and thus result in increased G_{CELL} without a notable change in a RMP.

In this study, 5-HT neurons in Tph2$^{-/-}$ mice displayed increased density of HCN channels when compared with littermates, suggesting that increased density of HCN channels may contribute to the higher G_{CELL} in Tph2$^{-/-}$ mice. However, since the difference was rather small and there was no significant correlation between the HCN channel-mediated depolarizing sag and G_{CELL}, increased HCN channel conductance does not seem to be a principal underlying mechanism. The observed difference in G_{CELL} could have been in part due to the increased cell surface area in Tph2$^{-/-}$ mice, since the difference in specific G_{CELL} (which accounts for the cell surface area) across the genotypes was less pronounced than that of G_{CELL}. (compare Figure 1C and F). Since the observed difference can at least in part be explained by the difference in somatic surface areas and since there were no changes in firing behavior, we did not further search for the underlying mechanism.

The observed differences in subthreshold electrophysiological properties and somatic surface areas in Tph2$^{-/-}$ mice might have been a caused directly by the lack of autoregulatory 5-HT action on 5-HT neurons, but they might also be an indirect consequence of the lack of CNS 5-HT. Namely, 5-HT has an important neurodevelopmental role via its effect in projection areas (reviewed in Daubert and Condron (2010), Lesch and Waider (2012) and, for Tph2$^{-/-}$ mice, in Mosienko et al. (2015)). Tph2$^{-/-}$ mice display abnormalities in brain development, such as reduced number of noradrenergic neurons in the locus coeruleus and lower norepinephrine content (Gutknecht et al., 2012), reduced density of GABAergic interneurons in the basolateral amygdala (Waider et al., 2013) and abnormal wiring of neuronal circuits in projection areas (Migliarini et al., 2012). Furthermore, the lack of the CNS 5-HT in Tph2$^{-/-}$ mice also leads to abnormalities in general development, such as growth retardation and increased mortality in the first weeks of postnatal life (Alenina et al., 2009; Narboux-Nême et al., 2013).

It has been well documented that 5-HT autoregulates expression and activity of neurotransmitter specific proteins in 5-HT neurons. For example, the absence of the CNS 5-HT in Tph2$^{-/-}$ mice leads to upregulation of 5-HT$_{1A}$ and 5-HT$_{1B}$ autoreceptors (Gutknecht et al., 2012), whereas the excess of extracellular 5-HT in Sert$^{-/-}$ mice leads to their downregulation (Fabre et al., 2000). In contrast, our findings suggest that 5-HT neuron firing activity is independent of endogenous 5-HT synthesis. Thus, changes in 5-HT specific proteins in 5-HT neurons are subject of homeostatic autoregulation by endogenous 5-HT, while changes in ion channels underlying pacemaking activity of 5-HT neurons appear to be notably less autoregulated.

An important consequence is that changes in expression or activity of ion channels of 5-HT neurons is expected to substantially influence the output of 5-HT system and thus may potentially lead to 5-HT system-related disorders. Similarly, in the treatment of neurodevelopmental and psychiatric disorders in which 5-HT system dysfunction is implicated, pharmacologic or genetic manipulation of 5-HT neuron ion channels should produce a more resilient change in 5-HT system functioning (a desirable outcome of the treatment) compared with analogous manipulation of 5-HT specific proteins. This hypothesis is supported by the study by Heurteaux and Colleagues (2006), who showed that genetic inactivation of the Kcnk2 gene, encoding a background K^+ channel, causes a notable increase in firing activity of DRN 5-HT neurons and leads to resistance to depression-like behavior in animal models. Similar behavioral effects were shown in Kcnk9 knockout mice (Gotter et al., 2011). In conclusion, our findings indicate that intrinsic electrophysiological properties of 5-HT neurons are independent of the level of 5-HT, suggesting that ion channels underlying 5-HT neuron activity can be pharmacologically targeted to produce an increase in firing and 5-HT release resistant to 5-HT dependent adaptive mechanisms.

Role of funding source

Funding for this study was provided by the University of Florence, the Deutsche Forschungsgemeinschaft (SFB TRR 58/A5 and Research Training Group RTG 1253/2), the European Community (EC: AGGRESSOTYPE FP7/No. 602805); O. Baytas was recipient of a fellowship from the ERASMUS Student Mobility for Placement Programme; A. Montalbano is recipient of a fellowship from the Regione Toscana and Aziende Chimiche Riunite Angelini Francesco A.C.R.A.F. SpA (POR CRO FSE 2007-2013: 5-HT@DRUGeMOOD). Mice are a product of European Union 6th Framework Program grant (LSHM-CT-2004-503474-NEWMOOD). The funding sources had no further role in study design; in the collection, analysis and interpretation of data; in the writing of the report; and in the decision to submit the paper for publication.

Contributors

Boris Mlinar designed the study, analyzed the electrophysiological data and wrote the first draft of the manuscript; Alberto Montalbano performed the electrophysiological recordings *in vitro* and morphological measurements; Mario Barbieri performed the recordings *in vivo*; Jonas Waider generated the eGFP/Tph2$^{-/-}$ mice;

Jonas Waider and Ozan Baytas performed the immunohistochemical labeling and channel expression determination; Renato Corradetti and Klaus-Peter Lesch contributed to the interpretation of the data and final manuscript. All authors contributed to and have approved the final manuscript.

Conflict of interest

The authors declare no conflict of interest.

Acknowledgment

The authors thank V. Bargelli for excellent technical support at the animal facility.

Appendix A. Supplementary material

Supplementary data associated with this article can be found in the online version at http://dx.doi.org/10.1016/j.euroneuro.2015.08.021.

References

Alenina, N., Kikic, D., Todiras, M., Mosienko, V., Qadri, F., 2009. Growth retardation and altered autonomic control in mice lacking brain serotonin. Proc. Natl. Acad. Sci. USA 106, 10332–10337.

Araragi, N., Mlinar, B., Baccini, G., Gutknecht, L., Lesch, K.P., Corradetti, R., 2013. Conservation of 5-HT1A receptor-mediated autoinhibition of serotonin (5-HT) neurons in mice with altered 5-HT homeostasis. Front. Pharmacol. 4, 97.

Audero, E., Mlinar, B., Baccini, G., Skachokova, Z.K., Corradetti, R., Gross, C., 2013. Suppression of serotonin neuron firing increases aggression in mice. J. Neurosci. 33, 8678–8688.

Booij, L., Tremblay, R.E., Szyf, M., Benkelfat, C., 2015. Genetic and early environmental influences on the serotonin system: consequences for brain development and risk for psychopathology. J. Psychiatry Neurosci. 40 (1), 5–18.

Borroto-Escuela, D.O., Narvaez, M., Pérez-Alea, M., Tarakanov, A. O., Jiménez-Beristain, A., Mudó, G., Agnati, L.F., Ciruela, F., Belluardo, N., Fuxe, K., 2015. Evidence for the existence of FGFR1-5-HT1A heteroreceptor complexes in the midbrain raphe 5-HT system. Biochem. Biophys. Res. Commun. 456, 489–493.

Branchereau, P., Chapron, J., Meyrand, P., 2002. Descending 5-hydroxytryptamine raphe inputs repress the expression of serotonergic neurons and slow the maturation of inhibitory systems in mouse embryonic spinal cord. J. Neurosci. 22, 2598–2606.

Crespi, F., 2009. Apamin increases 5-HT cell firing in raphe dorsalis and extracellular 5-HT levels in amygdala: a concomitant in vivo study in anesthetized rats. Brain Res. 1281, 35–46.

Daubert, E.A., Condron, B.G., 2010. Serotonin: a regulator of neuronal morphology and circuitry. Trends Neurosci. 33, 424–434.

del Burgo, L.S., Cortes, R., Mengod, G., Zarate, J., Echevarria, E., Salles, J., 2008. Distribution and neurochemical characterization of neurons expressing GIRK Channels in the rat brain. J. Comp. Neurol. 510, 581–606.

Eaton, M.J., Staley, J.K., Globus, M.Y., Whittemore, S.R., 1995. Developmental regulation of early serotonergic neuronal differentiation: the role of brain-derived neurotrophic factor and membrane depolarization. Dev. Biol. 170, 169–182.

Fabre, V., Beaufour, C., Evrard, A., Rioux, A., Hanoun, N., 2000. Altered expression and functions of serotonin 5-HT1A and 5-HT1B receptors in knock-out mice lacking the 5-HT transporter. Eur. J. Neurosci. 12, 2299–2310.

Galter, D., Unsicker, K., 2000. Sequential activation of the 5-HT1 (A) serotonin receptor and TrkB induces the serotonergic neuronal phenotype. Mol. Cell. Neurosci. 15, 446–455.

Gotter, A.L., Santarelli, V.P., Doran, S.M., Tannenbaum, P.L., Kraus, R.L., Rosahl, T.W., Meziane, H., Montial, M., Reiss, D.R., Wessner, K., McCampbell, A., Stevens, J., Brunner, J.I., Fox, S.V., Uebele, V.N., Bayliss, D.A., Winrow, C.J., Renger, J.J., 2011. TASK-3 as a potential antidepressant target. Brain Res. 1415, 69–79.

Gutknecht, L., Araragi, N., Merker, S., Waider, J., Sommerlandt, F. M., Mlinar, B., Baccini, G., Mayer, U., Proft, F., Hamon, M., Schmitt, A.G., Corradetti, R., Lanfumey, L., Lesch, K.P., 2012. Impacts of brain serotonin deficiency following Tph2 inactivation on development and raphe neuron serotonergic specification. PLoS One 7, e43157.

Gutknecht, L., Kriegebaum, C., Waider, J., Schmitt, A., Lesch, K.P., 2009. Spatio-temporal expression of tryptophan hydroxylase isoforms in murine and human brain: convergent data from Tph2 knockout mice. Eur. Neuropsychopharmacol. 19, 266–282.

Gutknecht, L., Waider, J., Kraft, S., Kriegebaum, C., Holtmann, B., Reif, A., Schmitt, A., Lesch, K.P., 2008. Deficiency of brain 5-HT synthesis but serotonergic neuron formation in Tph2 knockout mice. J. Neural. Transm. 115, 1127–1132.

Hajós, M., Allers, K.A., Jennings, K., Sharp, T., Charette, G., Sík, A., Kocsis, B., 2007. Neurochemical identification of stereotypic burst-firing neurons in the rat dorsal raphe nucleus using juxtacellular labelling methods. Eur. J. Neurosci. 25, 119–126.

Hajós, M., Gartside, S.E., Villa, A.E.P., Sharp, T., 1995. Evidence for a repetitive (burst) firing pattern in a sub-population of 5-hydroxytryptamine neurons in the dorsal and median raphe nuclei of the rat. Neuroscience 69, 189–197.

Hajós, M., Sharp, T., Newberry, N.R., 1996. Intracellular recordings from burst-firing presumed serotonergic neurones in the rat dorsal raphe nucleus in vivo. Brain Res. 737, 308–312.

Heurteaux, C., Lucas, G., Guy, N., El Yacoubi, M., Thümmler, S., Peng, X.D., Noble, F., Blondeau, N., Widmann, C., Borsotto, M., Gobbi, G., Vaugeois, J.M., Debonnel, G., Lazdunski, M., 2006. Deletion of the background potassium channel TREK-1 results in a depression-resistant phenotype. Nat. Neurosci. 9, 1134–1141.

Huether, G., Thömke, F., Adler, L., 1992. Administration of tryptophan-enriched diets to pregnant rats retards the development of the serotonergic system in their offspring. Dev. Brain Res. 68, 175–181.

Jacobs, B.L., Azmitia, E.C., 1992. Structure and function of the brain serotonin system. Physiol. Rev. 72, 165–229.

Lesch, K.P., Waider, J., 2012. Serotonin in the modulation of neural plasticity and networks: implications for neurodevelopmental disorders. Neuron 76, 175–191.

Migliarini, S., Pacini, G., Pelosi, B., Lunardi, G., Pasqualetti, M., 2012. Lack of brain serotonin affects postnatal development and serotonergic neuronal circuitry formation. Mol. Psychiatry 18, 1106–1118.

Miyazaki, K., Miyazaki, K.W., Doya, K., 2011. Activation of dorsal raphe serotonin neurons underlies waiting for delayed rewards. J. Neurosci. 31, 469–479.

Mlinar, B., Montalbano, A., Baccini, G., Tatini, F., Berlinguer Palmini, R., Corradetti, R., 2015. Nonexocytotic serotonin release tonically suppresses serotonergic neuron activity. J. Gen. Physiol. 145 (3), 225–251.

Mosienko, V., Beis, D., Pasqualetti, M., Waider, J., Matthes, S., Qadri, F., Bader, M., Alenina, N., 2015. Life without brain serotonin: reevaluation of serotonin function with mice deficient in brain serotonin synthesis. Behav. Brain Res. 15, 78–88.

Please cite this article as: Montalbano, A., et al., Cellular resilience: 5-HT neurons in Tph2$^{-/-}$ mice retain normal firing behavior despite the lack of brain 5-HT. European Neuropsychopharmacology (2015), http://dx.doi.org/10.1016/j.euroneuro.2015.08.021

Ruijter, J.M., Ramakers, C., Hoogaars, W.M., Karlen, Y., Bakker, O., van den Hoff, M.J., Moorman, A.F., 2009. Amplification efficiency: linking baseline and bias in the analysis of quantitative PCR data. Nucleic Acids Res. 37, e45.

Narboux-Nême, N., Angenard, G., Mosienko, V., Klempin, F., Pitychoutis, P.M., Deneris, E., Bader, M., Giros, B., Alenina, N., Gaspar, P., 2013. Postnatal growth defects in mice with constitutive depletion of central serotonin. ACS Chem. Neurosci. 4, 171–181.

Rumajogee, P., Vergé, D., Hanoun, N., Brisorgueil, M.J., Hen, R., Lesch, K.P., Hamon, M., Miquel, M.C., 2004. Adaption of the serotoninergic neuronal phenotype in the absence of 5-HT autoreceptors or the 5-HT transporter: involvement of BDNF and cAMP. Eur. J. Neurosci. 19, 937–944.

Sakai, K., 2011. Sleep-waking discharge profiles of dorsal raphe nucleus neurons in mice. Neuroscience 197, 200–224.

Sharp, T., Bramwell., S.R., Clark., D., Grahame-Smith, D.G., 1989. In vivo measurement of extracellular 5-hydroxytryptamine in hippocampus of the anaesthetized rat using microdialysis: changes in relation to 5-hydroxytryptaminergic neuronal activity. J. Neurochem. 53, 234–240.

Sharp, T., Bramwell, S.R., Grahame-Smith, D.G., 1990. Release of endogenous 5-hydroxytryptamine in rat ventral hippocampus evoked by electrical stimulation of the dorsal raphe nucleus as detected by microdialysis: sensitivity to tetrodotoxin, calcium and calcium antagonists. Neuroscience 39, 629–637.

Talley, E.M., Solorzano, G., Lei, Q., Kim, D., Bayliss, D.A., 2001. Cns distribution of members of the two-pore-domain (KCNK) potassium channel family. J. Neurosci. 21, 7491–7505.

Trulson, M.E., Jacobs, B.L., 1979. Raphe unit activity in freely moving cats: correlation with level of behavioral arousal. Brain Res. 163, 135–150.

Vandesompele, J., De Preter, K., Pattyn, F., Poppe, B., Van Roy, N., De Paepe, A., Speleman, F., 2002. Accurate normalization of real-time quantitative RT-PCR data by geometric averaging of multiple internal control genes. Genome Biol. 3 (7) RESEARCH0034.

Waider, J., Araragi, N., Gutknecht, L., Lesch, K.P., 2011. Tryptophan hydroxylase-2 (TPH2) in disorders of cognitive control and emotion regulation: a perspective. Psychoneuroendocrinology 36 (3), 393–405.

Waider, J., Proft, F., Langlhofer, G., Asan, E., Lesch, K.P., Gutknecht, L., 2013. GABA concentration and GABAergic neuron populations in limbic areas are differentially altered by brain serotonin deficiency in Tph2 knockout mice. Histochem. Cell Biol. 139, 267–281.

Washburn, C.P., Sirois, J.E., Talley, E.M., Guyenet, P.G., Bayliss, D. A., 2002. Serotonergic raphe neurons express TASK channel transcripts and a TASK-like pH- and halothane-sensitive K^+ conductance. J. Neurosci. 22, 1256–1265.

Whitaker-Azmitia, P.M., Azmitia, E.C., 1986. Autoregulation of fetal serotonergic neuronal development: role of high affinity serotonin receptors. Neurosci. Lett. 67, 307–312.

Whitaker-Azmitia, P.M., Azmitia, E.C., 1989. Stimulation of astroglial serotonin receptors produces culture media which regulates growth of serotonergic neurons. Brain Res. 497, 80–85.

Wu, M.F., John, J., Boehmer, L.N., Yau, D., Nguyen, G.B., Siegel, J. M., 2004. Activity of dorsal raphe cells across the sleep-waking cycle and during cataplexy in narcoleptic dogs. J. Physiol. 554, 202–215.

Please cite this article as: Montalbano, A., et al., Cellular resilience: 5-HT neurons in Tph2$^{-/-}$ mice retain normal firing behavior despite the lack of brain 5-HT. European Neuropsychopharmacology (2015), http://dx.doi.org/10.1016/j.euroneuro.2015.08.021